Korean Journal of Chemical Engineering
https://doi.org/10.1007/s11814-024-00256-5

REVIEW ARTICLE

Nanoparticle Doped Polymers for Radiation Shielding: A Review

Anupama V. Joshi[1] · K. Shastry[2] · Gagana Velur[1] · Bhoomika R. Holla[1]

Received: 17 April 2024 / Revised: 8 August 2024 / Accepted: 11 August 2024

Abstract
Radiation-shielding is essential in fields involving storage and transport of radiation active material, such as medicine and nuclear engineering. The risk of radiation spill is a source of constant concern with its potential impact on local environment and life. Radiation spills that occur in laboratory are considered minor and containment of radiations in such cases using conventional techniques is not practical. Current practice involves using a suitable chemical absorbent, cleaning the spill region using agents and requires monitoring the spill region regularly for activity. Although this technique is effective in managing minor/laboratory grade spills, it requires careful application and constant monitoring before the area can be deemed safe for work. In this paper, we provide a detailed review of the radiation-shielding properties of polymer nanocomposites and their fabrication. The paper outlines radiation-shielding mechanisms, measurement of radiation attenuation, and factors that influence radiation attenuation. The review also compares analytical attenuation measurement methods against experimental methods. This review would be helpful in not only understanding the underlying energy transfer mechanism, but also aid in exploring polymer nano-composite materials as a viable green option for containing medium to low-level radiation spills.

Keywords Shielding · Gamma rays · Neutron radiation · Nanoparticles · HDPE · Composites

Introduction

Radioactivity is the phenomenon of spontaneous disintegration of an unstable atomic nucleus to a stable configuration through emissions in the form of radiations (alpha, beta, gamma, neutron, etc.). In general, radiation can be categorized as either low or high energy depending on its ionization capacity [1]. In the current context, ionization is the process wherein an atom loses a loosely bound electron. This loss of electron is contingent upon the energy available in the system. For most part, non-ionizing radiation does not cause harm as it does not have sufficient energy to strip electrons off the atoms of a material. Examples of such radiation are microwaves and infrared radiations. Photons of high energy (gamma, X-rays), electrons (beta), and neutrons (due to their heavy mass) are capable of ionizing materials due to their high penetrating power and ability to cause atomic level changes in matter. Alpha particles can be defined as Helium atoms that have been stripped of their electrons, hence giving their + 2 positive charges. A single alpha particle ejected at high speed from a nucleus travels up to 4 cm in air before gaining two electrons and forming helium atom. Typically, alpha particles have high ionization capability and very poor penetrating power. A beta particle is basically a high-speed electron ejected from a decaying nucleus. Like alpha particles, beta particles also cause the formation of ions through interaction with matter. Fast-moving electrons that make up beta radiation have higher penetrating power than alpha radiation because of their smaller size. Gamma rays and neutrons are two of the most harmful ionizing radiations. Gamma radiations are pure electromagnetic waves that result as a byproduct of radioactive decay of nuclei. These radiations have high penetrating power and larger scattering cross sections. Free neutrons resulting either from nuclear fusion, fission, or isotope bombardment are known as neutron rays and have similar penetrating power and scattering cross section to gamma rays. Widespread applications of radioactivity have been found in fields like healthcare, archeology, mining, space exploration, military, and electricity production. Most of these applications call for the use of liquid radioactive materials and require serious considerations during

✉ Anupama V. Joshi
anupamavj@rvce.edu.in

[1] Department of Chemical Engineering, RV College of Engineering, Bangalore, India

[2] Department of Physics, RV College of Engineering, Bangalore, India

Published online: 18 August 2024

transport and handling. A fundamental consequence while dealing with radioactive materials and devices is the persistent concern of spill and contamination leading to serious runoff effects on the neighboring environment.

Radiation-shielding is an area that requires attention and the need to fill any gaps in shielding technology [2]. Radiation spills are incidents causing the release of radioactive materials into the environment due to accidents, human error, natural disasters, or malfunctioning of nuclear failsafe mechanisms. These spills can occur in nuclear power plants, research laboratories, industrial facilities, or during transportation of radioactive materials. Spills could be classified as either major or minor depending on the type and quantity of release. While major spills are generally accounted as radiation accidents, minor spills are small-scale radioactive contamination in hospitals, laboratories, and transportation of radioactive medical/industrial isotopes and radioactive waste. In cases of radiation spills, the response protocol includes impact mitigation measures like evacuation, measurement and monitoring of radiation levels and decontamination.

The increasing use of ionizing radiation for diagnostic and therapeutic purposes, particularly in higher-dosage procedures like computed tomography (CT) and interventional radiology, raises serious safety and health issues for both patients and medical staff. According to a study by Salerno and colleagues, just 35% of medical professionals who dealt with radiological diagnostics were aware of their risks and properly trained to handle spills [3]. In addition to exposure from medical and industrial techniques, radiation exposure also rises as a result of insufficient protection and human error [4].

Therefore, a method to shield against these harmful radiations needs to be made available as a primary safety measure and regulation. Protecting people, animals, and the environment from the harmful effects of ionizing radiation, especially high-energy electromagnetic radiation like gamma, neutron or X-ray, is the general aim of radiation protection. Consequently, it is essential to create materials with strong radiation-shielding properties [5]. This formed a strong motive to critically review the state-of-the-art on radiation-shielding and the use of nanoparticles/nanocomposites in radiation-shielding.

Radiation Shielding

Nuclear decay is a process wherein an unstable nucleus spontaneously emitting energy in the form of radiation(s) and eventually decaying into daughter nuclei which have more stable configurations. The nature of the radiations emitted during the decay process is in the form of high-energy sub-atomic particles and electromagnetic radiations [2]. Depending on its energy, radiation can be categorized into either ionizing or non-ionizing radiation. While non-ionizing radiation cannot penetrate deep into matter and hence loses its energy through both coherent /incoherent scattering and excitations of the orbital electrons, ionizing radiation on the other hand has the capability to penetrate deep into matter and has sufficient energy to strip electrons/atoms from matter causing considerable damage. The rate of such energy loss depends on the energy of incident radiation, density, and atomic composition of the matter through which it is passing. The differentiation between directly and indirectly ionizing radiations is based on the radiation's specific ionization. Specific ionization is defined as the number of ion pairs formed per unit path length for a given radiation [6, 7]. Alpha particles have high specific ionization and a relatively short penetration range in matter (a few centimeter in air and only fractions of a millimeter in tissue) owing to their double charge and slow velocity. On the other hand, beta particles have a much lower specific ionization as compared to alpha particles and in general exhibit greater range in tissue. As an example, energetic beta particles from Phosphorus-32 have a maximum range of seven meters in air and eight millimeters in tissue. The low-energy betas from Hydrogen-3, on the other hand, are stopped by only six millimeters of air or six micro-meters of tissue [7].

Examples of indirectly ionization radiations are gamma rays, X-rays, and neutrons, their lack of charge makes them unable to impart direct impulse to orbital electrons. Further, gamma and X-rays are part of the electromagnetic spectrum and proceed through the matter until there is a chance of interaction with matter (sub-atomic particle) [8]. If the sub-atomic particle is an electron, it may receive enough energy to be ionized, causing further ionization through direct interactions with other electrons. Indirectly ionizing radiations (e.g., gamma, X-rays, and neutrons) depend on chance encounters with electrons in matter and hence do not have finite ranges [9, 10]. In addition to gamma, alpha, and beta particles, a nuclear decay also emits fast neutrons. A neutron has a mass thousand times greater than an electron and hence possesses greater kinetic energy. These high-energy neutrons can transfer their kinetic energy through collisions with matter in a process called moderation. This process is most effective if the collisions occur with particles of similar mass [11]. After initial collisions, the neutrons are slowed down to the same average energy as the matter being interacted with, thereby the neutrons have a much greater chance of interacting with a nucleus leading to the material becoming either radioactive or cause radiation to be given off from the material. The two principal factors that influence the amount of ionization in a material are the radiation energy and the type of interacting material. For a given material, ionization levels will vary with varying levels of incident radiation energy. The three principal mechanisms

through which a material can get ionized are the Photoelectric Effect, Compton Effect, and Pair Production.

Photoelectric effect is a single-step process dominant between energies from 10 to 500 keV. During this process, the incident photon is absorbed completely by an orbital electron and ejected from the material. The minimum energy required to eject this electron from the material must be equal to the sum of binding energy and the work function of the material. The electrons that are ejected from the material due to the incident photon are referred to as photoelectrons. The closer the electrons are to the nucleus, the greater is the energy required to eject the electrons from the atom. The photoelectric equation is given by

$$E_{\mathrm{k}} = hv - E_{\mathrm{b}} - \varphi, \tag{1}$$

E_{k} is the kinetic energy of the photoelectron, hv is the energy of the photon, E_{b} is the binding energy of the energy level, and φ is the work function of the material. Therefore, in principle, the maximum energy of a photo-electron emitted from the outermost shell of a material surface is given by

$$E_{\mathrm{k}} = hv - \varphi. \tag{2}$$

Compton effect or scattering occurs between the energy ranges of 50 keV to 3 MeV. It is also referred to as inelastic scattering because the energy of the scattered photon is greater than the energy of the incident photon. Though this process can occur with the nucleus of the material, it is usually attributed to interactions involving the electrons of the material. There exists an overlap in the energies of Compton and photoelectric effects. At lower energies, photoelectric effect dominates Compton effect and the vice versa occurs at higher energies. Compton effect is the most dominant transition between the energies of 100 and 150 keV. Since not all of the photon's energy is utilized during the scattering of the electron. energy, there is energy left over to cause further ionization in the material.

$$\Delta\lambda = \frac{h}{m_o c}(1 - \cos\theta), \tag{3}$$

$\Delta\lambda$ is the change in wavelength, m_o is the mass of the electron, θ is the angle through which the photon is scattered, c is the photon energy.

In the case of pair production, the initial photon energy is as high as 1.02 MeV and above. Pair production is the strongest type of interaction between radiation and matter and does not involve orbital electrons; instead, the interaction is between the electromagnetic field of the atom and the photon. The incoming photon whose energy is in the range of a few MeV's is converted into a matter–antimatter pair (electron–positron) moving in different directions, away from each other. The positron being the antimatter of electron annihilates with the electrons in the material and generates two photons of energy 511 keV. During their journey through matter, the photons lose their energy and cause subsequent ionization in the form of Compton effect, and finally leading to photoelectric effect and total absorption. Equations (4) and (5) represent conservation of energy and momentum in pair production process (Fig. 1).

$$E_{\mathrm{photon}} = E_{\mathrm{electron}} + E_{\mathrm{positron}}, \tag{4}$$

$$pc_{\mathrm{photon}} = pc_{\mathrm{electron}} + pc_{\mathrm{positron.}} \tag{5}$$

In addition to ionization due to photons, we need to consider sub-ionization due to liberated electrons. Sub-ionization is a kind of cascading process where the energy liberated diminishes after every consecutive interaction till the energy is below the emission threshold. In the sub-ionization process, the atoms are not ionized, but the orbital electrons are excited to higher energy states and eventually release low-energy electromagnetic radiation. All high-energy photons like X-rays, gamma rays, and UV rays undergo similar transitions and contribute to a very small fraction of the total mass of the material. Therefore, it is important to understand the underlying ionizing mechanisms to choose the right material suitable for radiation-shielding.

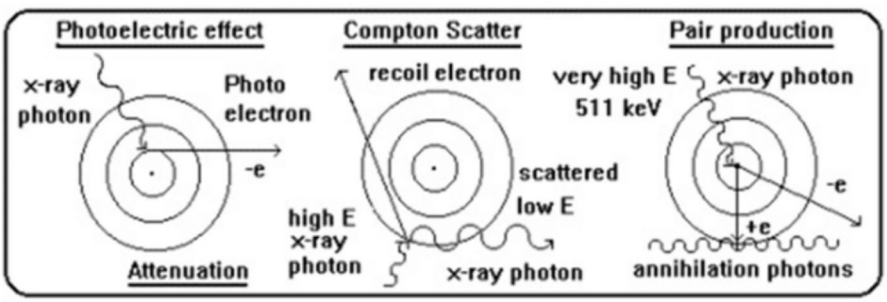

Fig. 1 Schematic representation of Photoelectric Effect, Compton Effect, Pair Production [12]

Radiation Shielding Parameters

In order to be considered as an efficient radiation-shielding material, parameters, such as material density, linear and mass attenuation coefficient, photon mean path, half-value layer, and radiation protection efficiency, are to be measured [13]. This section provides an insight into the relevance of these parameters with respect to radiation-shielding.

Linear attenuation coefficient (LAC) is the probability per unit path length that a photon of given energy will interact with the material. The value of this parameter varies based on factors, such as the energy of the incident photons, the density of the material, and its atomic number. The linear attenuation coefficient is calculated using Beer–Lambert law with the following equation:

$$I = I_o e^{-\mu x}, \tag{6}$$

where I and I_o are the intensities of the attenuated and incident photon rays, μ is the linear attenuation coefficient and x is the path length. If a material has high value of linear attenuation coefficient, it indicates that the material is a good radiation shield.

Mass attenuation coefficient is the material's ability to attenuate the intensity of a beam of electromagnetic radiation as it passes through the material. It considers the characteristics of the material, such as its density and atomic composition, as well as the energy of the incident photons. Mass attenuation coefficient can be calculated mathematically by dividing the linear attenuation coefficient by the mass density of the material.

$$\left(\frac{\mu}{\rho}\right)_c = \sum_i w_i \frac{\mu}{\rho}, \tag{7}$$

where w_i is the weight fraction and (μ/ρ) is the mass attenuation coefficient of the material. By comparing the mass attenuation coefficients of different materials, it becomes possible to identify materials that are more suitable for radiation-shielding purposes. Materials with higher attenuation coefficients are generally preferred for shielding application.

Photon mean path is defined as the average distance that a photon travels in a medium before experiencing an interaction. It is expressed as a distance, such as centimeters or meters. It represents an average value photon may travel varying distances before interacting. It is calculated using the formula:

$$\lambda = \frac{1}{\mu}. \tag{8}$$

The mean path length incorporates both absorption and scattering processes. Absorption refers to the complete absorption of photons by the medium, whereas scattering involves the redirection of photons without complete absorption. Both processes contribute to reducing the distance a photon can travel before being affected.

Table 1 Radiation-shielding parameters for lead

Parameter	Value
Linear attenuation coefficient at 1.25 MeV [24]	0.545 cm^{-1}
Mass attenuation coefficient at 1.25 MeV [24]	0.0332 cm g^{-2}
Half-value layer at 1.173 MeV [25]	1.2 cm
Mean free path at 2 MeV [26]	1.915 cm

The thickness of the shield required to reduce the intensity of the incident radiation by 50% after passing through it is known as half-value layer. It is calculated using the formula:

$$\mathrm{HVL} = \frac{0.693}{\mu}, \tag{9}$$

where μ is linear attenuation coefficient. The HVL value is dependent on the energy of the incident radiation. Different energies of radiation will have different HVL values for a given material. Higher-energy radiation typically requires thicker HVL values to achieve the same level of attenuation. If a material has low value of HVL, it is considered as a good radiation shield.

Effective atomic number is a weighted average of the atomic numbers of the constituent elements of a material based on their relative proportions and their respective atomic interactions with radiation. The atomic numbers of the elements present in the material are weighted according to their relative abundances. Elements with higher atomic numbers and greater contributions to the electron density have a larger impact on the effective atomic number. It can be calculated using the formula:

$$Z_{\mathrm{eff}} = \frac{\sum_i f_i A_i \left(\frac{\mu}{\rho}\right)_i}{\sum_i f_i \frac{A_i}{Z_i} \left(\frac{\mu}{\rho}\right)_i}, \tag{10}$$

where f_i is the ratio of ith element number to total element number in the material, A_i and Z_i indicate the atomic weight and atomic number of ith element in the material.

While effective atomic numbers provide a useful approximation of material behavior, it is important to note that it does not capture all the complexities of radiation-matter interactions. The detailed atomic structure, elemental

Table 2 Radiation-shielding parameters for lead at 59.5 keV

Parameter	Value
Linear attenuation coefficient at 59.5 keV	0.593 cm^{-1}
Mass attenuation coefficient at 59.5 keV	0.289 cm g^{-2}
Half-value layer at 59.5 keV	1.168 cm
Effective atomic number at 59.5 keV [27]	10.42

Table 3 Mean free path of gamma rays between 356 and 1332 kev in different compositions of concrete

Sample	Mean free path (cm)			
	356 keV	662 keV	1173 keV	1332 keV
Ordinary	4.3048	5.5803	7.3314	7.8186
Hematite–serpentine	3.9216	5.1948	6.8493	7.2993
Ilmenite–limonite	3.4483	5.5662	6.0277	6.4350
Basalt–magnetite	3.2467	4.2753	5.6338	6.0060
Ilmenite	2.8604	3.7950	5.0125	5.3504

arrangement, and molecular bonding effects are not fully accounted for. Scattering cross section is a measure of the probability of scattering occurring during an interaction between a particle or photon and a target. It represents the effective area available for scattering to take place. Scattering cross section can be measured for both elastic scattering (where the energy of the scattered particle or photon remains unchanged) and inelastic scattering (where the energy changes).

Inelastic mean free path gives the average distance traveled by the particle through the material before losing energy. When a photon enters a material, its energy diminishes due to one or more successive inelastic scattering/Compton scattering leading to the generation of secondary photons. This leads to the accumulation of energy within the material and is dependent on the photon intensity. Gamma buildup factor is a dimensionless number greater than one that considers secondary photons produced in the material. It is a measure of the ability of a material to attenuate gamma rays and is used to calculate the dose rate (amount of radiation absorbed or delivered per unit time) of gamma radiation in a material. In radiation-shielding design, it is used to determine the thickness of the shielding material required to reduce the dose rate of gamma radiation to a safe level. Usually, a mathematical technique called the G-P fitting is employed to calculate the effective buildup factor (EBF) for the polymer samples [12, 13]. The G-P fitting function is calculated using a geometric progression formula that factors the energy of the gamma rays, atomic number of the material, and the thickness of the material.

Tables 1 and 2 provide the values of radiation-shielding parameters measured for Lead and concrete respectively. Higher value of linear or mass attenuation corresponds directly to better shielding. Generally, materials with high density and atomic number are better gamma radiation shields as they have higher probability for atom–photon interaction and lower inelastic mean free path. Table 3 shows the inelastic mean free path of gamma rays between 356 and 1332 keV in different compositions of concrete [14].

The underlying distinctions in the physics of interaction with materials by gamma and neutron radiation define type and nature of shielding. A heavy substance like lead or iron is effective at attenuating gamma rays, while a hydrogen-containing substance like water, not particularly good at attenuating gamma rays is however efficient at shielding neutrons. Lead (Pb) with its high density and atomic mass of 207.2 amu has a mass attenuation coefficient of 5.64 cm^2/g [15], for an incident radiation of 100 keV. Other high atomic number materials suitable for gamma radiation-shielding are tungsten, dysprosium, gadolinium, bismuth, and barium [20, 21]. Conventionally, different mixtures of concrete are used for both neutron and gamma ray shielding [22, 23]. It has a linear attenuation coefficient of 0.224 to 0.256 cm^{-1} [20]. Lead-based shielding, though effective, has severe detrimental effects on the environment. There are not only primary health risks to the person handling lead, but also the chances of secondary transfer to others involved [20, 25, 26]. There is irrefutable proof of fatal compromise of a patient's immunity, reproductive, and nervous system due to prolonged lead exposure [23]. To create shielding aprons and covers, lead powder is mixed with fabrics. However, because pinholes form in polymer–metal composites, incident photons can enter polymer regions, which causes a problem with the shielding capabilities.

Material becomes heavier than necessary because extra material must be employed to achieve adequate protection due to these pinholes in the polymer matrix [28]. Depending on how they are used or stored, tiny cracks may form in lead aprons, thereby compromising on the radiation efficiency [5]. Radiation-shielding materials have even been developed using cement. But transportation of such materials is more challenging due to their massive weight and vast volume. Additionally, a major issue is the difficulty in the integration of the various shielding materials after they have been destroyed or disintegrated [29].

Materials like lithium, boron, and gadolinium have excellent neutron absorption properties while, materials like barite, hydrogen and water are excellent neutron scattering agents [30]. Since hydrogen has a neutron scattering length of 6.67 fermi-meter, polymer compounds with high hydrogen content like polyethylene and polyester act as efficient scatterers of neutron radiation. Boron-10, which is a (20–80) combination of 10B and 11B isotopes, has a very high neutron absorption cross section of 767 barn [31]. The thermal neutron capture reaction of 10B is given as follows:

$$10B + n \rightarrow [11B] * \rightarrow 4He(1.47\text{MeV}) + 7Li(0.84\text{MeV}) + \gamma(0.48\text{MeV})$$

$$10B + n \rightarrow 4He(1.79\text{MeV}) + 7Li(1.01\text{MeV}).\ [16]$$

Therefore, a combination of suitable materials consisting of polymers and nanocomposites that can effectively mitigate the gamma and neutron radiation needs to be developed.

Analytical Methods for Radiation Shielding Calculations

Analytical methods for radiation-shielding calculations refer to statistics-based approaches that provide approximate solutions to radiation transport and attenuation equations. These methods are often used for quick estimations or initial design evaluations. Point Kernel Method, Build-up Factor Method, Exponential Attenuation Method, and Semi-Empirical Methods are a few examples.

The point kernel method, also known as Knoll's formula, approximates the radiation dose rate at a point in space based on the source characteristics and material properties. It assumes a point source and homogeneous shielding materials. The method uses point kernels, which are pre-calculated factors that describe the radiation transport from a point source to a point in space. While it is a simplified approach that provides quick estimations, it has several limitations, such as not accounting for heterogeneity, air gaps, different layers, or density, within in shield [32]. This can potentially lead to inaccurate dose rate estimations and has limited applicability to complex geometries. Knoll's formula is best suited for simple structures like point or line sources and cannot calculate accurate results for irregular shapes, multiple sources, or complex shield arrangements. Since the formula assumes direct radiation paths from the source to the point of interest, it does not account for scattering effects which can significantly affect the dose distribution in the shielded region, particularly at larger distances from the source. The result of this neglect can lead to either under or overestimation of the dose rates [33]. A fundamental drawback of Knoll's formula is that it is valid for only gamma and X-ray energy ranges. As different radiation types require specific transport equations and cross-sectional data, an empirical formula like Knoll's cannot provide accurate or reliable results for neutron and charged particles [34]. Build-up Factor Method bases its calculations on the factor by which the total value of a quantity (photon fluence, exposure, or dose) being assessed at a point of interest exceeds the value associated with only primary radiation in a material due to multiple scattering and secondary particle production. The approximation to the radiation attenuation is done by introducing a build-up factor (determined from tabulated data and empirical formula) that accounts for the reduction in radiation transmission. Exponential Attenuation Method is based on Beer–Lambert's law and assumes that the radiation decays exponentially as it penetrates deeper into a material. The intensity of the radiation/charged ion or particle decreases exponentially with distance and is proportional to the material's linear attenuation coefficient and distance traversed.

A more practical approach to simulating radiation-shielding that can factor in the different variables and give accurate results is either based on Monte Carlo random sampling codes, such as FLUKA, GEANT (Geometry And Tracking), and MCNP (Monte Carlo N-Particle), or on extensive repositories/ resources like National Institute Standards and Technology (NIST) database. These databases rather provide specific software packages, offer data, models, and tools for simulating shielding geometries, multi-particle interactions and trajectories. Since FLUKA, GEANT, and MCNP are computationally intensive codes, simulations involving large and complex shielding designs can be time-consuming. The memory requirements for running either FLUKA, GEANT, or MCNP simulations can be substantial, thereby limiting its practicality for certain applications on less-powerful computing systems [35–37]. As the nature of geometry gets more complex the computing requirement also increases furthermore, the packages have specific shortcomings while simulating high-energy neutrons [37]. Agostinelli et al. compared GEANT's performance with experimental data for high-energy neutron shielding simulations and found discrepancies between the simulated and measured data for mean path length correction, the mean lateral displacement for multiple scattering process at small angles [38]. While MCNP can handle complex geometries, it requires careful modeling and parameterization. Generating accurate and efficient geometry models, particularly for complex shield configurations, can be challenging and time-consuming. Incorrect or overly simplified geometry modeling can lead to inaccuracies in dose calculations [38]. Simulations based on NIST and MCNP can be plagued by issues of inconsistency in data due to incomplete repositories or databases. The uncertainties in the databases can lead to significant uncertainties for specific isotopes, reactions, or energy ranges. It is important to consider the limitations and uncertainties associated with the chosen nuclear data library [39, 40].

GEANT4 is a software platform used for simulation of the passage of particles through matter. An event generator, detector simulation, reconstruction, and analysis are the four main components of the software. Geant4 software was created as the foundation for the simulation component, and it was necessary for it to have clear interfaces with other components and to offer pieces that could be used by them. Modularity, adaptability, and a clear, user-verifiable implementation of physics are further design needs. The user can select only the components they require, thanks to GEANT's modular architecture. Geometry and materials, particle interaction in matter, tracking management, digitization and hit management, event and track management, visualization and visualization framework, and user interface are the primary areas of the simulation for the passage of particles through matter. The

development of class categories with coherent interfaces and accompanying working groups with well-defined responsibilities for each category followed naturally from the emergence of these domains. Additionally, it gave rise to the idea of a "toolkit," which suggests that a user may create their program at compile time using components either provided by themselves or taken from the toolkit. Geant4 uses cutting-edge software engineering methods to meet important criteria for functionality, modularity, extensibility, and openness. The "Booch Methodology" was the foundation for the architectural design techniques, which took an iterative approach with incremental refinement of user requirements, architectural, and detailed design.

Singh et al. [41] used MCNP-4C simulation code to calculate the mass attenuation coefficient, μ/ρ values for various polymers (polypropylene, perspex, Bakelite, Teflon, polyethylene, polycarbonate, nylon 6–6, and PMMA) and water for photon energies ranging from 59.5 to 1332.5 keV. For chosen gamma ray energies, the radiation sources were defined as planar, collimated beams, mono-energetic sources, with uniform distribution of radioactivity. All simulation data were presented with less than 1% error, and the results were compared to practical and theoretical XCOM results from the literature. Similar research by Vahabi et al. [42] produced results that were in excellent agreement with Singh's data. The mass attenuation coefficient for specific polymers was calculated in this work using the MCNP4C tool. The XCOM program's predictions and experimental data were compared with the simulation findings for gamma ray energy ranging from 59.5 to 1332.5 keV. The findings suggested that the geometry employed in this investigation was practical for computing the mass attenuation coefficients of the polymers, particularly for low-energy photons, and that the results were in good agreement with the XCOM data. It was determined that the MCNP4C model utilized in this work was a good contender for additional material properties and could be used in situations when no comparable experimental data exists, especially for polymers. The FLUKA Monte Carlo code was used in the study by Sharma et al. [43] to examine the gamma ray interaction parameters of various polymeric materials, including polytetrafluoroethylene, bakelite, polyethylene terephthalate, polypropylene, polysulfone, polystyrene, polyethylene, natural rubber, polymethyl methacrylate, and polyvinyl chloride. Several characteristics linked to radiation interactions were reported by the inquiry, including the mass attenuation coefficient, relaxation length, tenth-value layer, half-value layer, electronic cross section, atomic cross section, effective atomic number, and effective electron density. With a relative deviation of less than 1%, the FLUKA Monte Carlo code's results were in good agreement with the XCOM standard reference database. The study concluded that FLUKA can be an alternate method for estimating different interaction characteristics of polymeric materials, particularly when an experiment is difficult to set up. In terms of the selected polymers, polyvinyl chloride and polytetrafluoroethylene perform best as shielding materials between 59.5 and 1332.5 keV, respectively. Mirji et al. [20] investigated the mass attenuation coefficients of commonly used synthetic polymers, including polyethylene, polystyrene, polycarbonate, polyvinyl alcohol, polyvinyl chloride, polyethylene terephthalate, polyvinyl pyrrolidone, polytetrafluoroethylene, polypropylene, and polymethyl methacrylate, using second-order polynomial equation and the logarithmic interpolation method for gamma photon energy ranging from 14.4 keV up to 1332 keV. With all the polymeric materials taken into consideration, with photon energy ranging from 300 to 2000 keV, the second-order polynomial equation fits the NIST data fairly well. The outcomes of these techniques aid in comparing data from experiments and other theoretical techniques. The calculated mass attenuation coefficients of different polymers are useful for determining other radiation-related characteristics and for choosing the appropriate shielding material.

The mass attenuation coefficients for water and soft tissue for gamma rays with energies between 0.2 and 2 MeV were calculated in this study by Vahabi et al. [44]. The buildup factor (BF) values were introduced with the use of the MCNP simulation program and a co-centric multilayer model. The outcomes were compared to data that had already been published and to the ANSI/ANS-6.4.3 standard. In comparison to the slab geometry model of MCNP, the used model demonstrated improved predictions of BF values at specific penetration depths. The highest discrepancy was seen at 10 mfp and 0.5 MeV, and the BF values derived by simulation were in good agreement (10% difference) with the ANSI/ANS-6.4.3 standard. The simulation's uncertainties were less than 5%, which helped to partially explain why the simulation's conclusions differed from normal ones. The suggested model suggested the possibility of further research into deeper penetration and higher photon energy for computing BF values.

The gamma ray attenuation characteristics of a few thermoplastic polymers were assessed by More et al. in their study [13]. The purpose of the study was to determine how well these polymers worked in nuclear medicine applications at various photon intensities. Using a NaI (Tl) detector, the WinXCom program, and MCNPX simulation, the mass attenuation coefficient (m) of the chosen polymer samples was determined between the photon energies of 122 and 1332 keV. The other relevant parameters, such as the linear attenuation coefficient, total molecular, atomic, and electronic cross sections, effective atomic number, effective electron density, relaxation length, HVL, and TVL, were then estimated using the m values. The findings demonstrated that, as shown in Fig. 2, the experimental findings and the values of the attenuation parameters

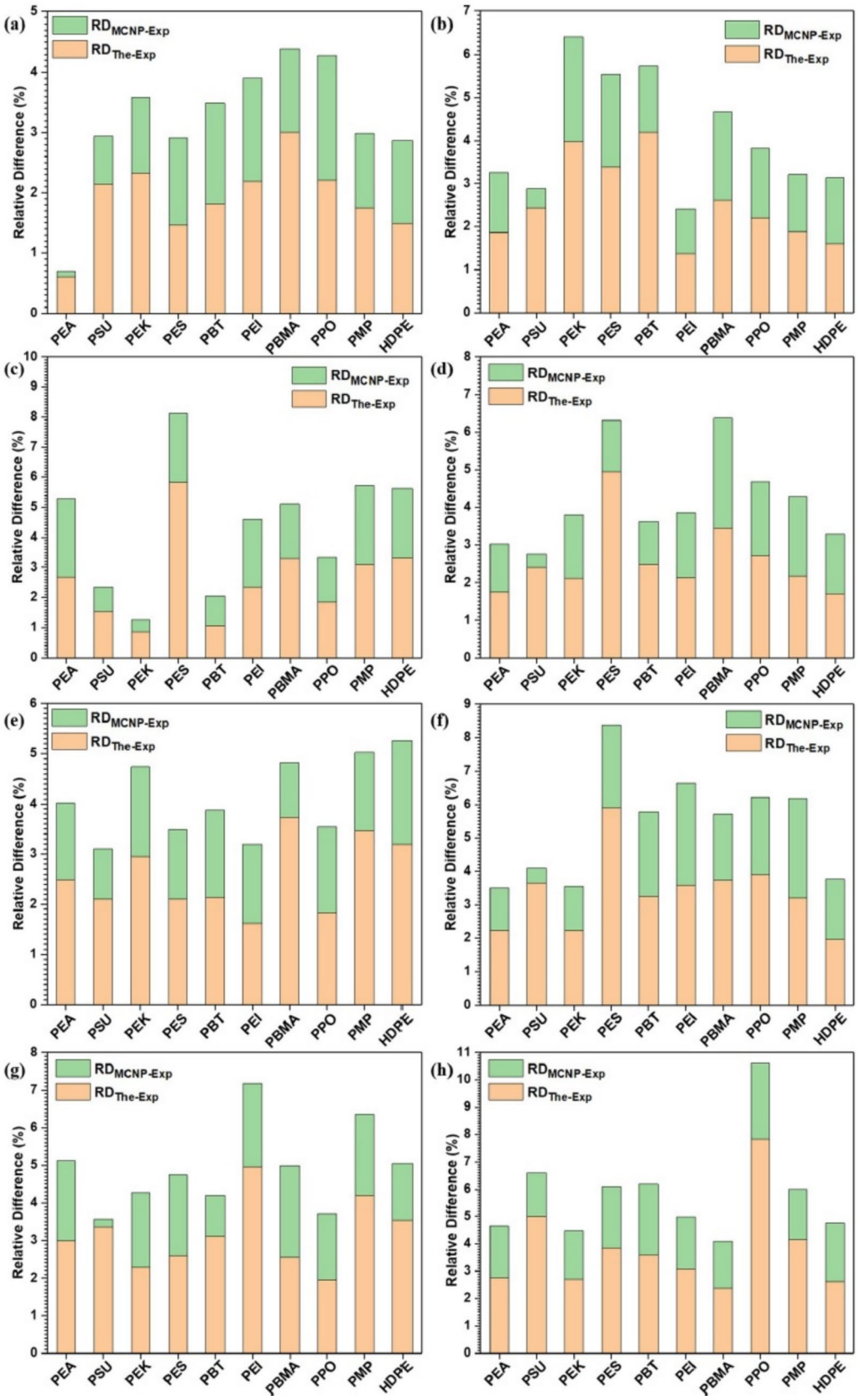

Fig. 2 Plot of Relative differences (%) of theoretical and simulated μm with respect to experimental values for **a** 122, **b** 356, **c** 511, **d** 662, **e** 840, **f** 1173, **g** 1257 and **h** 1332 keV [13]

agreed satisfactorily. In contrast to the values acquired by WinXCom, the experimental values of m were discovered to be closer to those computed by MCNPX. The efficiency of well-known thermoplastic polymer materials in nuclear medicine applications at various photon energy was also examined and reviewed in the study.

Though there are some challenges in effectively simulating radiation-shielding, an important fact to be considered is that Monte Carlo-based software packages and databases are ever evolving and are potent tools in simulating particle/radiation transport and shielding. Regular updates and patches of such software make them very relevant and can replicate the experimental details to very high accuracy. In their investigation, Biswas et al. [42] determined the mass attenuation coefficient (μ_m) of polyboron, a locally created shielding material, and compared it to the results of the WinXCom code for photon energies between 0.001 and 20 MeV. From the resulting mm values, the linear attenuation coefficients (μ) and relaxation lengths (l) were also determined, and their fluctuations with photon energy were displayed. The research discovered that the shielding materials' density, chemical make-up, and photon energy all had a significant impact on the values of μ_m, μ, and l.

According to the findings, polyboron's μm and m values at low photon energies were higher than those of pure polyethylene and borated polyethylene but lower than those of regular concrete and water. All the sample materials exhibited around the same millimeter values at the intermediate photon energy range (0.125–6 MeV). Additionally, the research revealed that polyboron exhibited the same relaxation duration (l) across the full photon energy range. For a few typical gamma sources, the transmission curves are presented together with the total mass attenuation coefficient (μm), linear attenuation coefficient (m), half-value layer (HVL), and tenth-value layer (TVL) of the five sample materials. The study's findings help demonstrate the viability of polyboron as a biological shielding material and the necessity for additional research to create an empirical model for calculations involving neutron and gamma ray transport.

Monte Carlo simulations have a strong online presence that provides regular software support and beginner assistance to get started in coding; their online repositories are regularly updated and can be accessed with ease. In certain instances, there are cloud computing services provided at a premium to conduct the necessary simulations. With such ease of use, Monte Carlo software and packages are widely used and accepted for simulations not just for radiation-shielding, but also in bio-medical engineering, high-energy physics, and nuclear engineering applications.

Preparation Nanoparticles for Radiation Shielding

Metal and metal oxide nanoparticles have been extensively researched for various applications because of the functional enhancement the nanomaterials offer owing to their high surface area and increased surface interactions. Nanomaterials have been popularly used as a dopant in various polymer materials to introduce or enhance their functional properties.

A similar experiment was performed on Bismuth by Muhammed and the team which agreed with the previous team's result. Bismuth nanoparticles showed higher attenuation coefficient and lower HVL [43]. It is frequently observed that nanoforms of materials show better radiation-shielding than bulk material. In Table 4, various metals and metal oxides used for radiation-shielding have been reviewed. Different forms of radiation, gamma, IR, X-rays, and neutron rays were used and radiation-shielding of various nanomaterials was investigated [45–55].

The table suggests that nanoparticles show radiation-shielding properties for gamma, neutron, X-rays, and neutron rays. Parameters like HVL, shielding efficiency, and attenuation coefficients were used to measure shielding depending on the requirements. But there are a few drawbacks to be kept in mind. Nanoparticles, particularly Boron Nitride, possess high surface energy and agglomerate which leads to poor dispersion in a polymer matrix. This can have adverse effects on the composite and leads to defects and degradation of the polymer matrix [48].

Polymeric nano-composite materials are being explored for use in radiation-shielding because of their low density, ease of processing, multi-functionality, and shielding ability. Polymer bases like polypropylene, ethyl vinyl acetate impregnated with metal oxide nanofillers form polymer composites that have shown radiation-shielding properties [50].

Effect of Size, Shape, Loading, and Particle Wetting on Radiation Shielding

The size of the nanoparticles can affect the shielding ability of the polymer composites against high-energy and neutron radiation. Smaller nanoparticles can provide better shielding performance as they have a higher surface area-to-volume ratio, which increases the probability of interactions with the gamma rays. When radiation interacts with nanoparticles, it undergoes scattering, changing its direction, and reducing its ability to penetrate through

Table 4 Nanoparticles used for radiation shielding

Dopant	Matrix	Radiation	Summary
Cesium-doped tungsten trioxide	Epoxy composite	Infrared ray	Blocked wavelength ranging from 800 to 1200 nm 0.021 wt% of Cs_xWO_3 NPs resulted in 24.5% decrease in IR intensity [61]
Cerium dioxide	ZrO_2 fiber	Infrared ray	Coating of 18 nm CeO_2 on ZrO_2 fiber shield the fiber from radiative heat waves and exhibited stronger infrared extinction capability [62]
Bismuth	Cellulose nanofiber	X-ray	The X-ray attenuation was 96.6% at 8% mass of Bi NPs for 60 kV X-ray beam [28]
Bismuth titanate ($Bi_4Ti_3O_{12}$)	Epoxy composite	X-ray	The matrix of 2 mm thickness achieves the highest X-ray attenuation coefficient of 97% at 80 kV and 95% at 100 kV. This was equivalent to 0.35 mm Pb but with half its weight [63]
Ferric oxide (Fe_2O_3)	Mortar	Gamma ray	Mortar with 25% Fe_2O_3 NPs was reported to have the lowest photon transmission. The HVL decreased from 1.223 cm to 1.074 cm, demonstrating that an increase in Fe_2O_3NPs concentration increased gamma ray shielding capabilities [58]
Lead oxide	CMC[a] and PVP[b]	Gamma ray	The nanocomposite showed a high attenuation coefficient with Cs-137 as a source of gamma radiation. The transmitted radiation decreases with increase in concentration of PbO_2 NPs[64]
Copper oxide	Recycled HDPE	Gamma ray	The mass attenuation coefficient value decreases with increase in CuO NPs concentration [65]
Lead oxide	HDPE	Gamma ray	PbO nano-filler showed 8.3% more MAC when compared to bulk PbO. Bulk PbO at 50 wt% showed significant increase in MAC [44]
Zinc oxide	No polymer matrix	Gamma ray	ZnO nanoparticles of 50 nm showed the lowest transmission factor value, high linear attenuation coefficient and decrease in HVL, TVL, and MFP [55]
Zirconium oxide (ZrO_2)	Lead borate glass	Gamma ray	The mass attenuation coefficient decreased with increase in ZrO_2 NPs concentration when irradiated with 662, 1173, and 1332 keV of photon energy and increased for 356 keV of photon energy [45]
Titanium boride	No polymer matrix	Gamma ray	NPs were of size 42 nm and the attenuation coefficient was 0.238 cm^{-1} and HVL was 2.91 cm [43]
Boron and gadolinium	Ultra-high molecular weight polyethylene	Neutron	6 layers of UHMWPE along with a core sheet of Resin + 3%boron nano-powder showed 99.64% radiation shielding, whereas Resin + 3% Gd NPs of 700 nm showed 99.4% shielding [46]
Boron nitride	High-density polyethylene	Neutron	Hexagonal BN nanocomposite was tested, and high attenuation coefficients were obtained with very low secondary radiation. Shielding efficiency of 1.3 was obtained with 8 cm thick nanocomposite [47]

[a] *CMC* carboxy methyl cellulose

[b] *PVP* polyvinyl pyrrolidone

the composite. As the size of nanoparticles decreases, the scattering effect becomes more pronounced, resulting in improved radiation-shielding. But it is imperative that there is an optimal size range for nanoparticles in terms of radiation-shielding efficiency. Extremely small nanoparticles, especially particles less than 100 nm, may agglomerate or form clusters due to dominant intermolecular van der Waals interactions, leading to reduced scattering and shielding effectiveness [54].

Rashad et al. studied the influence of size of ZnO and MgO nanoparticles on gamma and neutron rays shielding using FLUKA. The size range of the nanoparticles with which he worked is 50–70 nm. It was seen that semi-spherical ZnO particles of 50 nm size showed the highest mass attenuation coefficients [55].

Ran Li et al. studied the effect of particle size on gamma radiation-shielding property of gadolinium oxide dispersed epoxy resin matrix composite. Characterization using SEM showed that nano-particles are small flocculent-like particles. The influence of particle size on Gd_2O_3 becomes more noticeable at low particle concentrations. However, as the particle concentration increases, the size effect becomes less significant. This is because at higher particle concentrations, both micro- and nano-composites exhibit

a similar arrangement of particles, leading to a weakening of the size effect [56].

Particle wetting refers to the interaction between a solid particle and a liquid, specifically how the liquid spreads or adheres to the surface of the particle. It describes the degree to which the liquid can coat or cover the particle's surface. Wetting behavior has an indirect impact on the radiation-shielding capacity of polymer nanocomposites. Wetting depends on the energies (or surface tensions) of the interfaces involved such that the total energy is minimized [57]. The wetting properties of the polymer matrix affect the dispersion and distribution of the nanoparticles within the composite, which in turn, influence radiation-shielding [58]. When nanoparticles are well-wetted by the polymer matrix, they are more likely to form a uniformly dispersed composite. This leads to improved radiation-shielding properties. On the other hand, poor wetting can result in agglomeration or poor dispersion of the nanoparticles within the polymer matrix. This can create voids or regions with reduced nanoparticle concentration, leading to compromised radiation-shielding performance. A good wetting interface can promote strong adhesion and bonding, improving the overall mechanical integrity of the composite. This is important for maintaining the structure of the material during exposure to radiation, as exposure to radiation can degrade or damage the composite [54].

The shape of nanoparticles can also have a significant impact on the radiation-shielding properties of a polymer matrix. Different nanoparticle shapes can affect the scattering, absorption, and penetration of radiation, thereby influencing the overall radiation-shielding effectiveness of the composite material. Shruti Nambiar et al. took examples of carbon nanotubes (CNTs), Cement/concrete (spherical) and clay platelets to study the effect of shape of nanoparticles on radiation-shielding. Spherical nanoparticles have a symmetrical shape which allows for efficient scattering of radiation, as the incident radiation interacts with the nanoparticles from all directions. Additionally, spherical nanoparticles can have a high surface-to-volume ratio, enhancing their ability to absorb and scatter radiation. Nanoparticles with an elongated or rod-like shape increase the likelihood of multiple scattering events, leading to greater attenuation of radiation. Nanoparticles with a flat or plate-like shape, such as nanosheets or nanoplates have large surface area and flat geometry which enable effective absorption and scattering of radiation. Plate-like nanoparticles can also create barriers that hinder the penetration of radiation, providing additional shielding effectiveness [49].

Nanoparticle loading is usually expressed as a weight or volume fraction, indicating the percentage of nanoparticles in the polymer composite. It is important to note that there is an optimal loading range for nanoparticles in terms of radiation-shielding efficiency. Excessive nanoparticle loading can lead to agglomeration or clustering, which may result in poor dispersion, reduced scattering efficiency, or even increased radiation leakage through gaps between clusters. On the other hand, low nanoparticle loading in a polymer matrix may result in reduced scattering efficiency, limited absorption capacity, incomplete coverage, and weaker attenuation of secondary radiation.

Özdemira et al. performed attenuation tests on nano-lead oxide and EPDM (Ethylene–Propylene–Diene Monomer) to examine the response of the material under gamma ray irradiation. Dumbbell-shaped samples, manufactured in accordance with ASTM D412 Type C specifications, were subjected to various radiation doses. The samples contained lead oxide nanoparticles in concentrations of 1%, 5%, 10%, 15%, and 20% (w/w). Irradiation was performed using a Cobalt-60 source within a Gammacell 220 model irradiator. The total doses administered were 81, 100, and 120 kGy. These irradiation experiments aimed to assess the material's performance under the specified exposure conditions. Results for 81 kGy energy showed that at 10%, 15% and 20% weight percentage, the attenuation coefficients were 0.421, 0.532, and 0.607 cm^{-1}, i.e., it increased as the loading percentage increased [59].

Farnaz Nasehi et al. measured the mass attenuation coefficients of Polyacrylamide and ZnO composites using at 5%, 10%, 15%, and 20% weight percentages for 661.66 keV energy radiation using XCOM. The XCOM program is a tool applied for obtaining the total cross sections and attenuation coefficients for the incoherent and coherent scattering, photoelectric absorption, and pair production. The MAC was found to be 0.08217, 0.0817, 0.0813 and 0.0809 cm^2/g respectively. It can be observed that as loading increases, the attenuation coefficient decreases [60].

Polymer Composites and Nanocomposites as Radiation Shield

While the choice of nanoparticle is important, method of fabrication also plays a significant role while developing a radiation-shielding nanocomposite or a fabric. There are several methods like melt blending, in situ polymerization, solution compounding, knitting, or weaving that have been employed by researchers in the past to incorporate shielding additives in a polymer matrix or a fabric which is effective in minimizing the radiation emissions. Each technique has its distinct advantages and limitations which need to be tailored to specific applications and material requirements. The development of a universal method for making polymer composites depends on a variety of elements, including the equipment at hand, the overall cost, and the required properties of the finished product.

In in situ polymerization, nanofiller is added in the monomer or oligomer during polymerization due to which there is an increased chance of strong interaction of the additive with the polymer matrix [66]. Bagheri and team developed an unsaturated polymer composite incorporated with 10 wt%, 20 wt%, and 30 wt% lead oxide nanoparticles of size 0.1–0.2 µm and 5% montmorillonite nano-clay using in situ polymerization at room temperature. Then the mixture was ultra-sonicated for good dispersion of the fillers and removal of bubbles. Nano-clay particles improved the mechanical and thermal properties of the composite which was disrupted by lead particles. No appropriate dispersion of lead oxide particles with a concentration higher than 30% was attained using this approach. Linear and mass attenuation co-efficient were reported to increase with increase in filler concentration [67].

In solution compounding technique, the polymer is dissolved in a specific solvent and the radiation-shielding additive is added to the resulting solution. The solution is cast into a film or sheet and solvent is evaporated [68]. A polyvinyl alcohol, polyethylene glycol, polyvinyl pyrrolidinone composite with 2 wt%, 4 wt%, 6 wt%, and 8 wt% of Fe_3O_4 nanoparticles was developed with a thickness of 22–45 µm. The composite was irradiated with Cs-137 and the attenuation coefficient increased as wt% rose. Fe_3O_4 nanoparticles added to the polymer solution were found to agglomerate at lower concentrations of 2 wt%, 4 wt%. But as the concentration rose to 8 wt%, a network of nanoparticles was formed and the attenuation improved to 0.149 μcm^{-1} [69]. Mehrara and team emphasized the importance of temperature of solvent being used to dissolve the polymer. The developed a polycarbonate doped with varying wt% of Bi_2O_3 nanoparticles by first dissolving polycarbonate in boiling dichloromethane (39.6 °C) and then nanoparticles were to this solution by keeping the temperature of mixture above the boiling point and ultra-sonicated to ensure good dispersion of nanoparticles. When the nanocomposite was irradiated with gamma energy less than 140 keV, the rate of increase of mass attenuation co-efficient was high with 10, 20, and 30 wt% of the filler as shown in Fig. 1. But with further increase in filler concentration (40 wt% and 50 wt%) in the matrix, the rate of increase of mass attenuation co-efficient was slow due to agglomeration of nanoparticles [70]. The agglomeration of nanoparticles could also be avoided by coating the nanoparticles with LDPE. Despite these advantages, shielding polymer prepared with this technique requires the use of hazardous solvents, removal of solvent is a difficult process during mass production.

Melt blending involves the use of mixing devices like two-roll mill or three-roll mill (shown in Fig. 3) or an extruder to melt the polymer and filler together. The mixture is then cooled, solidified, and cast into a sheet. This is a simple, cost-effective, and co-friendly technique as no solvents are required and can easily be scaled up for large-scale production. This method cannot be employed for heat-sensitive polymers and there is no control over dispersion of the filler [68]. Huang et al. developed a nanocomposite of ethylene–propylene–diene monomer rubber with fillers, such as carbon black and ball-milled $PbWO_4$ powder of 200 nm ranging from 100 to 400phr. The fillers were mechanically stirred to achieve uniform dispersion and the composite was irradiated with Eu-155, Cs-137, and Co-60. Increase in $PbWO_4$ powder up to 400 phr increased the mass attenuation coefficient as seen in Fig. 4, but additional increase of powder lowered the matrix's tensile strength and elongation break due to a close packing of the powder. Hence, in

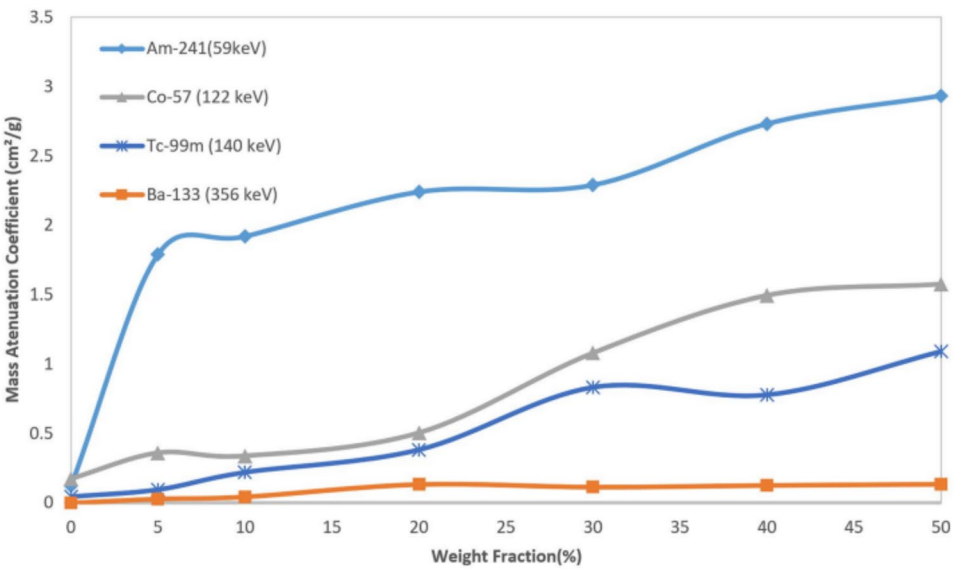

Fig. 3 Variation of mass attenuation co-efficient with different wt% of filler [70]

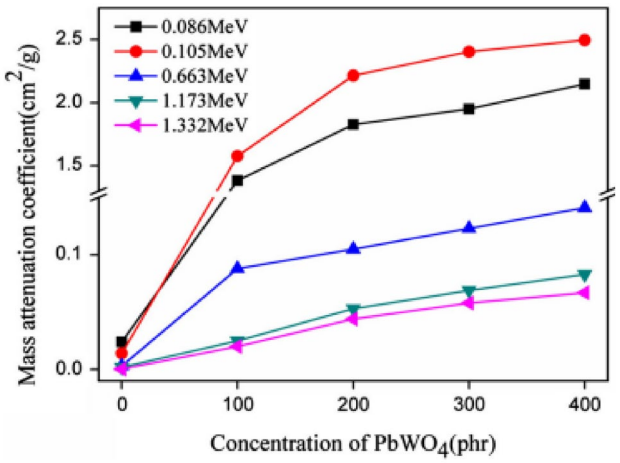

Fig. 4 Mass attenuation coefficient for different concentration of $PbWO_4$ powder [71]

order to achieve good attenuation properties, the filler content must be optimally chosen to obtain optimal interaction between the filler and the matrix [71].

Tohid and team developed polyvinyl chloride composite doped with 10 g, 20 g, and 40 g tungsten micro-particles using melt blending method. Linear attenuation coefficient increased with increase in tungsten micro-particle when irradiated with gamma ray of energy 662 keV, 1173 keV, and 1332 keV. Linear attenuation coefficient obtained with 40 g tungsten doping was comparable to lead, but the composite was much lighter when compared to an apron doped with lead [72].

Fabrics are bundles of fibers which have a specific property arranged and combined in either a 2-dimensional or 3-dimensional space depending on the thickness and size required. Fabrics are widely used in radiation-shielding applications due to their low density, flexibility, and designability. Fabrics can be divided into three different kinds depending on the mode of radiation protection and transmission line theory: electromagnetic (EM) shielding, EM wave absorbing, and EM wave transparency. EM shielding fabrics are made of materials that are highly conductive and reduce the intensity of EM energy transmitted by reflection. Such fibers can be developed by surface metallization, metal coating, and woven fabrics with conductive fibers. The bottom of EM wave absorbent fabrics is made of metal, which produces a powerful reflection. As a result, when radiation strikes a metal substrate, it reflects and falls on the fiber where it is absorbed. There are two different kinds of EM wave absorbent fabrics: coated and structural. Coated fabrics have absorbent coatings like graphite, carbon black, or magnetic compounds. Structural fabrics are made by weaving together strands of two fibers with different compositions (for example nickel–iron or carbon). The third type is EM

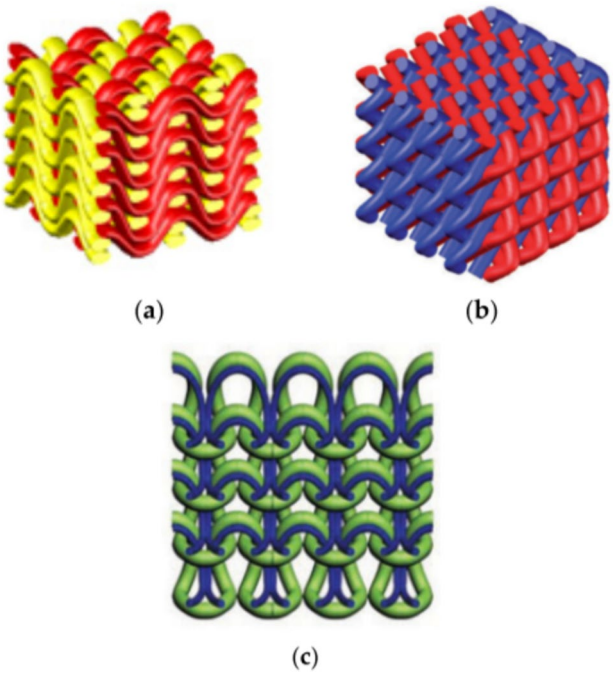

Fig. 5 **a** Woven fabric; **b** braided fabric, **c** knitted fabric [73]

wave transparent fabric mainly used in defense and military. Fabrics can be divided based on their structure as woven, braided, and knitted fabric as shown in Fig. 5 [73].

Shielding fibers are typically produced through the two primary methods of lamination and weaving. Lamination involves coating a non-woven fabric with a liquid shielding material that has been blended with a polymer, as opposed to weaving, which involves injecting the fabric with a shielding additive before weaving it.

Gholamzadeh and team coated fabric with 40 wt% micro- and nano-WO_3, Bi_2O_3, and PbO and irradiated it with Cs^{137}, a gamma source of 0.662 MeV. The attenuation co-efficient was the highest for fabric coated with 40% nano-PbO and the co-efficient increased with increase in filler material. At lower energy levels, nano-filler-coated fabric displayed better attenuation of gamma rays than micro-filler-coated fabric. Thus, this fabric-coating approach demonstrated that the technique could be used to create lightweight, flexible aprons [74].

A cotton polyester blend fabric was coated with 40 wt%, 50 wt%, and 60 wt% barite and irradiated with 662 keV, 1173 keV, and 1332 keV produced by ^{137}Cs and ^{60}Co. This barite coating absorbed the radiation and the linear attenuation co-efficient increased with increase in barite concentration on the fabric as shown in Fig. 6 [75].

Son J and team used twill-weaving method to weave yarn containing a filler (5wt% barium sulfate) and were able to achieve higher density of the shielding fiber in comparison to the fibers produced using plain weaving. Plain

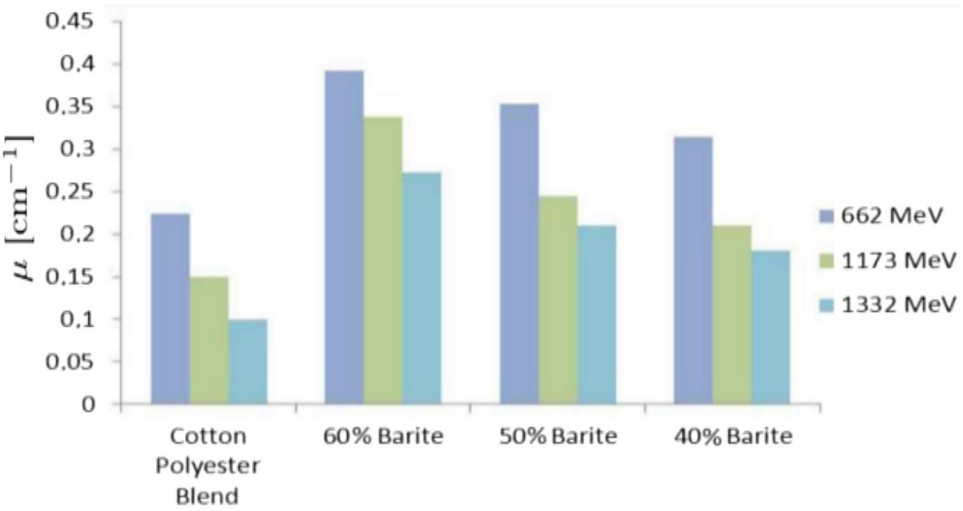

Fig. 6 Variation of linear attenuation co-efficient with different concentration of barite on fabric [75]

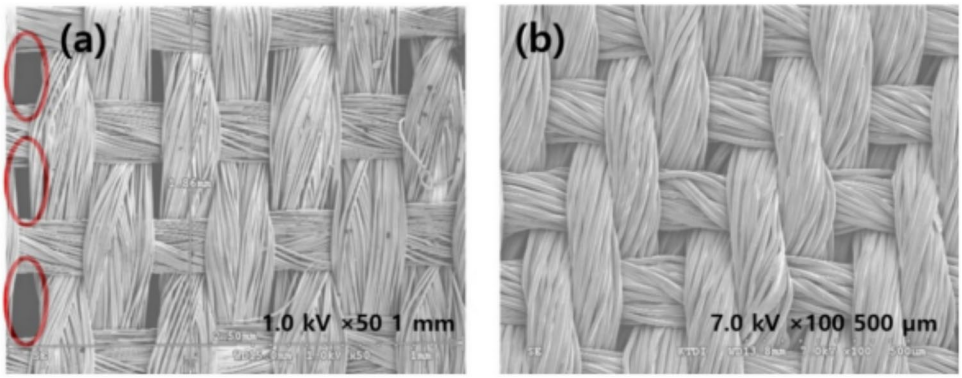

Fig. 7 **a** SEM image of pinhole in plain-woven fabric and **b** SEM image of twill-woven fabric [76]

woven fabrics produced pinholes and was less dense, but twill-woven fabrics used more yarn but did not produce any pinholes as shown in Fig. 7. When the two fabrics were exposed to X-ray of energy ranging from 40 to 120kVp, twill-woven fabric displayed higher radiation-shielding rate than the plain-woven fabric [76].

Polyester and stainless steel core yarn with cotton fiber as sheath material have been used to develop cellular woven fabrics. This fabric when irradiated with gamma source Am-241 showed a shielding effectiveness of 36.95% which was higher than the 3/1 twill-woven fabric. This was mainly due to the presence of stainless steel, which contains a heavy metal atom Fe, a good gamma radiation-shielding additive, being integrated within the yarn of the cellular fabric [77]. Because gamma shielding involves introducing heavy metal atoms into the fiber, such as lead or iron, and since this procedure is difficult as this fiber must withstand heavier atoms than itself, there are not many studies published on the use of woven fabrics as a gamma radiation shield.

Dispersing nanoparticles in a polymer matrix is reported to be a promising design as nanoparticles offer a large surface area-to-volume ratio. When a heavy atom is doped in a hydrogen-rich polymer matrix, it not only exhibits high attenuation of gamma radiation, but also has a large scattering cross section with respect to fast moving neutrons [37]. Size of the nanoparticle, their agglomeration tendencies, method of synthesis of the polymer nanocomposite must be taken into consideration while choosing a polymer and the nanofiller. Table 5 consolidated the polymer composites that have been used for radiation-shielding [35, 38–41].

Table 6 shows that radiation-shielding is dependent on the weight percentage of the micro- or nano-filler. There are also a variety of parameters that measure the radiation-shielding property of a polymer composite. It is important to set a standard parameter when comparing composites. Linear and mass attenuation coefficients have been seen to be the easiest to analyze. Therefore, in the rest of the discussions, we will be using these parameters.

HDPE polymer composites for radiation-shielding

High-density polyethylene (HDPE) is the most widely used polymer, even though several polymer composites are being made and tested for their shielding properties. HDPE is a

Table 5 Polymers with nanoparticles as fillers

Polymer	Filler	Results
Unsaturated polyester resin	Bismuth oxide	60% bismuth filler has resulted in higher attenuation coefficients over the bare polymer base at various gamma photon energies ranging between 80 and 1332 keV. the HVL, TVL and relaxation length decreased with increasing filler concentration, thus improving the shielding property while still being lighter conventional materials [50]
Ethylene vinyl acetate	Tungsten	Transmittance is 8% in 2 mm disk made of ethylene vinyl acetate filled with 70% tungsten when irradiated by Cs-137. This material was found to be elastic, soft and easily shapeable [51]
Natural rubber	Boron oxide	Boron carbide-loaded natural rubber subjected to thermal neutron radiation shielding showed the highest value of linear absorption coefficient of 0.34 cm^{-1} for the composite containing 20 phr of B_4C [52]
Polyethylene	Boron nitride	Neutron beam of energies up to 600 MeV. The polymer composite of 8 cm showed shielding efficiency of 1.15 whereas Al showed efficiency of 0.9 [47]
Polypropylene	Bismuth oxide	Micro- and nanoparticles were incorporated into polypropylene at different weight percentages. At 0.06 MeV, the highest linear attenuation coefficient was 4.1513 cm^{-1} for PP-50 m Bi_2O_3 [78]

Table 6 Comparison of mass attenuation coefficient (cm^2g^{-1}) of HDPE and different fillers at 59.53 keV

Filler	Type	MAC
No filler [30]	–	0.170
10% PbO [30]	Bulk	0.685
50% PbO [30]	Bulk	3.158
10% PbO [30]	NP	0.742
50% PbO [30]	NP	3.407
10% Bismuth [44]	Bulk	0.609
20% Bismuth [44]	Bulk	0.879
40% Bismuth [44]	Bulk	2.168
10% ZnO [45]	Bulk	0.318
20% ZnO [45]	Bulk	0.455
30% ZnO [45]	Bulk	0.579
40% ZnO [45]	Bulk	0.703
10% ZnO [45]	NP	0.397
20% ZnO [45]	NP	0.483
30% ZnO [45]	NP	0.636
40% ZnO [45]	NP	0.770

material that is heavily explored in this field due to its simplicity in manufacture, low cost, high chemical resistance, and great flexibility. It is effective in absorbing and dispersing radiation because of its high hydrogen content. In the following part, we have examined the radiation-shielding characteristics of HDPE polymer composites with various bulk and nano-fillers.

HDPE is a common polymer that possesses a number of desirable engineering qualities which include high mechanical ductility, chemical inertness, and superior wear performance. Even at high temperatures, HDPE can maintain their mechanical strength, and the addition of nano-fillers can significantly enhance their inherent characteristics [53]. Due to its high hydrogen concentration (11%) and high scattering power, polythene is an effective neutron moderator [30]. HDPE nano-composite loaded with Tungsten (W), Molybdenum sulfide (MoS_2), and boron carbide (B_4C) demonstrated that the flexible composite sheet of HDPE 45% (wt) tungsten provided comparable X-ray absorption to the non-flexible lead sheet but much lighter in weight [79]. Table 6 shows that lead oxide is the best filler to the HDPE matrix for gamma ray shielding. It showed a significant increase in mass attenuation coefficients of polymer composites with increasing filler loading (bulk and nano). Nano-lead oxide has a much higher mass attenuation coefficient compared to bulk with 3.407 cm^{-1} at 50% loading irradiated with 59.53 keV of energy. But lead oxide is a runoff material. Ecosystems contaminated with lead show a wide range of adverse effects. The next best material other than lead was found to be zinc oxide. Zainab Alsayed et al. studied the effect of loading 10%, 20%, 30%, and 40% of bulk and nano-zinc oxide to HDPE. The comparison shows that at 40% nano-zinc oxide showed the highest mass attenuation of 0.770 cm^{-1}. From Fig. 4, it can be seen that nano-fillers have a higher attenuation coefficient compared to bulk fillers at the same loading [13]. A potential gamma radiation shield was developed using recycled HDPE (R-HDPE) doped with copper oxide nanoparticles and phosphotungstic acid. This nanocomposite was prepared using compression-molding. First, R-HDPE was melted in a two-roll mixer running at a speed of 50 rpm at a temperature of 180 °C for 10 min. CuO NPs and phosphotungstic acid during the melting stage were continuously mixed for 15 min. This mixture was poured into stainless steel mold and hot-pressed using a hydraulic press at 180 °C for 15 min at 20 MPa and later cooled in water.

Using XCOM database as reference, the researchers concluded that as the photon energy increased, the mass attenuation coefficient decreased [17]. Mohamed et al. also used compression-molding technique to dope HDPE with bulk and nano-lead oxide particles. Similar result i.e., increase in mass and linear attenuation coefficient with increase in

weight fraction of lead nanoparticles and the coefficients decreased as the photon energy increased [18]. With the same technique, 10 wt%, 20 wt%, 30 wt%, and 40 wt% of micro-cadmium oxide and nano-cadmium oxide were dispersed in HDPE [19]. Researchers have developed nanocomposite of HDPE doped with bismuth oxide nanoparticles prepared by casting method [20] (Fig. 8).

Cellulose Acetate Nanocomposites

Cellulose acetate (CA) is a biodegradable and biocompatible polymer, typically made from wood pulp. It has excellent optical clarity, high toughness, and electrical insulation properties. CA finds various applications because of its ability to be easily casted using simple solvent casting methods. CA nanocomposite films have been tested for UV radiation-shielding in the past. Nusrat Jahan and team investigated the UV shielding capability of cellulose acetate/graphene oxide nanocomposites. The UV–VIS analysis revealed that visible light had an optical transparency of 76–99%, but UV radiation was significantly shielded as well [80].

Thus, it is important to see if CA has been used as a gamma radiation shield. Since CA is a degradable material, the effect of gamma irradiation on CA is of research interest. Limited research has been reported on the CA matrix using more than one filler as a shield. Very few papers could be found on the effects of mechanical properties of cellulose acetate exposed to gamma radiations.

Gamma radiation was discussed by Hanaa Kamal and her team as a way to enhance the mechanical and barrier qualities of cellulose acetate. They used 10 kGy gamma rays to irradiate the composite (CA/PEG/clay). When compared to un-irradiated films, it was observed that the tensile strength, elastic modulus, and elongation of the irradiated films were improved [81]. In another study, EL-Ashhab et al. assessed how gamma radiation affected the structural and physical characteristics of CA. The polymer was exposed to a cobalt-60 (50 kGy) source and the radiation caused random chain scission in cellulose acetate. It was also reported that the duration of exposure directly affects the quantity of scission, which in turn affects the kinetics of CA breakdown [82]. Between the two experiments, conflicting behavior is seen. One study claims that mechanical qualities improve, while the other found that gamma radiation accelerated the rate of CA breakdown. The work by Nusrat Jahan et al. suggested that UV shielding was significantly seen even though CA had good optical transparency. All of these observations point to the possibility of cellulose acetate as a gamma shield, which is yet to be tested.

Conclusions

Radioactive spills are a possibility even after meticulous adherence to safety protocols. Several processes and methods are followed to minimize the level of contamination depending on the severity of the spill. Current shielding techniques are based on run-off materials like lead, bismuth, etc. that can severely impact the local environment. Polymer materials with suitable nanoparticle combination can be used as effective radiation shields, thereby minimizing the risk of further contamination through run-off materials. It was found that hydrogen-rich polymers make for superior neutron shields and in comparison, to other similar polymers and natural rubber, HDPE demonstrated a higher mass attenuation coefficient; however, this is insufficient to protect against simultaneous gamma and neutron exposure. In combination with heavy nanoparticles, the efficacy of

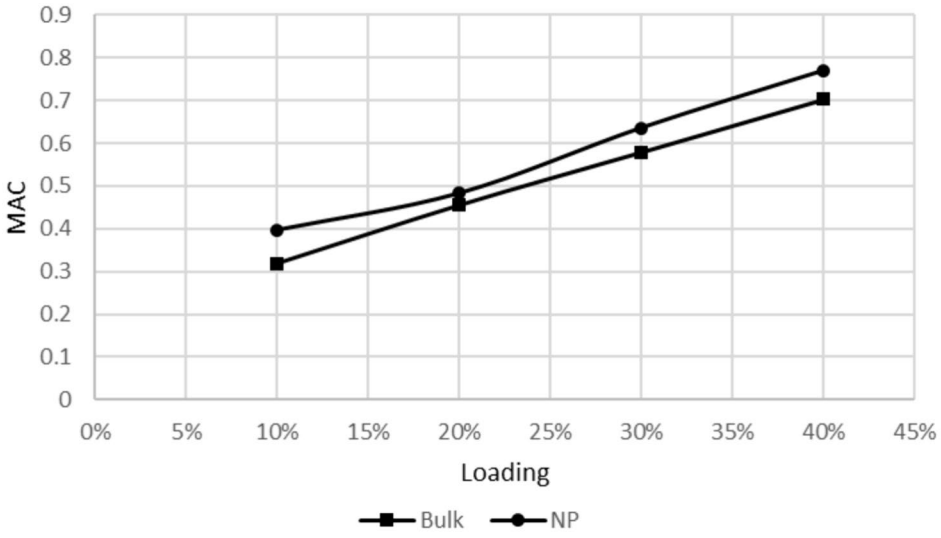

Fig. 8 Mass attenuation coefficients of HDPE with bulk and nano-zinc oxide fillers [49]

the polymer nanocomposite toward gamma and neutron radiation-shielding has been reviewed in detail. This review also details the LAC and MAC values for different combinations of polymers and corresponding fillers. The combination of HDPE with ZnO bulk/nanoparticles yielded positive results as a viable gamma shield. A major gap in the research highlighted in this review is that most radiation-shielding materials are either good at shielding gamma or neutron radiation, but not both. Furthermore, very few attempts have been made at understanding the high agglomeration and surface energy of boron nitride nanoparticles. A biocompatible alternative to radiation-shielding in the form of cellulose acetate was also discussed, and the serious research gaps in testing the viability of cellulose acetate as a suitable gamma and neutron shield was highlighted.

References

1. A. Cook, G.C. Meggitt, Radiological protection. Energy Dig. **8**(2), 16–19 (1979). https://doi.org/10.4324/9780203020746-18
2. J.K. Shultis, R.E. Faw, Radiation shielding technology. Health Phys. **88**(4), 297–322 (2005). https://doi.org/10.1097/01.HP.0000148615.73825.b1
3. A. Ploussi, E.P. Efstathopoulos, Importance of establishing radiation protection culture in Radiology Department. World J. Radiol. **8**(2), 142 (2016). https://doi.org/10.4329/wjr.v8.i2.142
4. S.C. Kim, Analysis of shielding performance of radiation-shielding materials according to particle size and clustering effects. Appl. Sci. (2021). https://doi.org/10.3390/app11094010
5. S.C. Kim, K.R. Dong, W.K. Chung, Medical radiation shielding effect by composition of barium compounds. Ann. Nucl. Energy **47**, 1–5 (2012). https://doi.org/10.1016/j.anucene.2012.04.014
6. E.B. Podgorsak, *Radiation physics for medical physicists* (Springer, Berlin, 2010). https://doi.org/10.1007/978-3-642-00875-7
7. D.A. Schauer, O.W. Linton, National Council on Radiation Protection and Measurements report shows substantial medical exposure increase. Radiology **253**(2), 293–296 (2009). https://doi.org/10.1148/RADIOL.2532090494
8. P. Croüail, F. Drouet, Survey on the implementation of the 'justification','optimisation' and 'limitation of doses' radiological protection principles in national regulations in Europe (February–May 2006), no. May 2006 (2006)
9. H. Bichsel, H. Schindler, H. Bichsel, H. Schindler, The interaction of radiation with matter. Part. Phys. Ref. Libr. (2020). https://doi.org/10.1007/978-3-030-35318-6_2
10. M.H. McKetty, The AAPM/RSNA physics tutorial for residents. X-ray attenuation. Radiographics **18**(1), 151–163 (1998). https://doi.org/10.1148/RADIOGRAPHICS.18.1.9460114
11. J. K. Shultis, R. E. Faw, Radiation shielding, p. 537.
12. Mechanism picture. http://img.chem.ucl.ac.uk/www/kelly/medicalxrays.html
13. C.V. More, Z. Alsayed, M.S. Badawi, A.A. Thabet, P.P. Pawar, Polymeric composite materials for radiation shielding: a review. Environ. Chem. Lett. (2021). https://doi.org/10.1007/s10311-021-01189-9
14. S. Singh, A. Kumar, D. Singh, K.S. Thind, G.S. Mudahar, Barium-borate-flyash glasses: as radiation shielding materials. Nucl. Instrum. Methods Phys. Res. Sect. B Beam Interact. Mater. Atoms **266**(1), 140–146 (2008). https://doi.org/10.1016/j.nimb.2007.10.018
15. S. Gopal, B. Sanjeevaiah, Gamma-ray attenuation coefficient measurements. Phys. Rev. A **8**(6), 2814–2818 (1973). https://doi.org/10.1103/PhysRevA.8.2814
16. R. Mirji, B. Lobo, Radiation shielding materials: a brief review on methods, scope and significance. Proc. National Conference on 'Advances in VLSI and Microelectronics', 27th January 2017; P.C. Jabin Science College, Huballi, India; ISBN 978-81-931806-8-6; Pages 96-100 JABINTRONICS-2017. https://www.researchgate.net/publication/317687481
17. N. Jamal AbuAlRoos, M.N. Azman, N.A. Baharul Amin, R. Zainon, Tungsten-based material as promising new lead-free gamma radiation shielding material in nuclear medicine. Phys. Med. **78**(August), 48–57 (2020). https://doi.org/10.1016/j.ejmp.2020.08.017
18. T.H.E.S. Problem, *The Penetrative Radiation of Concern in Reactors* (Elsevier, Oxford, 1982)
19. I.I. Bashter, Calculation of radiation attenuation coefficients for shielding concretes. Ann. Nucl. Energy **24**(17), 1389–1401 (1997). https://doi.org/10.1016/S0306-4549(97)00003-0
20. S. Özen, C. Şengül, T. Erenoğlu, Ü. Çolak, I.A. Reyhancan, M.A. Taşdemir, Properties of heavyweight concrete for structural and radiation shielding purposes. Arab. J. Sci. Eng. **41**(4), 1573–1584 (2016). https://doi.org/10.1007/s13369-015-1868-6
21. M. Ogawa, Y. Nakajima, R. Kubota, Y. Endo, Two cases of acute lead poisoning due to occupational exposure to lead. Clin. Toxicol. **46**(4), 332–335 (2008). https://doi.org/10.1080/15563650701816448
22. S.M. Hulbert, K.A. Carlson, Is lead dust within nuclear medicine departments a hazard to pediatric patients? J. Nucl. Med. Technol. **37**(3), 170–172 (2009). https://doi.org/10.2967/jnmt.109.062281
23. N.J. Abualroos, N.A. Baharul Amin, R. Zainon, Conventional and new lead-free radiation shielding materials for radiation protection in nuclear medicine: a review. Radiat. Phys. Chem. (2019). https://doi.org/10.1016/j.radphyschem.2019.108439
24. N. Defence, A. Kaduna, Determination of linear absorption coefficient for different materials absorbers of varying lengths first colliminator Radioactive source sodium iodide detector (NaI) Ratemeter (Decade Scaler Counter), **3**(8), 28–38 (2018)
25. J.K. Shultis et al., Gamma ray attenuation properties of common shielding materials. J. Non Cryst. Solids **305**(3), 529–534 (2005). https://doi.org/10.1016/j.jnoncrysol.2014.08.003
26. Y. Zuo, J. Zhu, S. Niu, A comparative study of empirical formulas for gamma-ray dose build-up factor in iron and lead materials. IOP Conf. Ser. Mater. Sci. Eng. (2018). https://doi.org/10.1088/1757-899X/439/2/022008
27. Gamma and Neutron Shielding Concrete.pdf.
28. Q. Li et al., Enhanced radiation shielding with conformal lightweight nanoparticle-polymer composite. ACS Appl. Mater. Interfaces **10**(41), 35510–35515 (2018). https://doi.org/10.1021/acsami.8b10600
29. J.W. Shin et al., Polyethylene/boron-containing composites for radiation shielding. Thermochim. Acta **585**, 5–9 (2014). https://doi.org/10.1016/j.tca.2014.03.039
30. S.A. Thibeault, J.H. Kang, G. Sauti, C. Park, C.C. Fay, G.C. King, Nanomaterials for radiation shielding. MRS Bull. **40**(10), 836–841 (2015). https://doi.org/10.1557/mrs.2015.225
31. H. Issard, Radiation protection by shielding in packages for radioactive materials. Safe Secur. Transp. Stor. Radioact. Mater. (2015). https://doi.org/10.1016/B978-1-78242-309-6.00009-5
32. G. Knoll, Radiation detection and measurement. 2010. [Online]. https://books.google.co.in/books?hl=en&lr=&id=4vTJ7UDel5IC&oi=fnd&pg=PA1&dq=Knoll,+G.+F.+(2010).+Radiation+Detection+and+Measurement+(4th+ed.).+John+Wiley+%

26amp%3B+Sons.&ots=VxHPBRxScB&sig=gbfM7k-oDgy1bvhmhEOSO1zDfdI. Accessed 4 Aug 2023
33. J. T.-F., E. Abstracts and undefined 1995, Atoms, radiation and radiation protection, infona.plJE TurnerFuel Energy Abstr. 1995•infona.pl,. [Online]. https://www.infona.pl/resource/bwmeta1.element.elsevier-65e1695c-2641-3f2c-b955-2e29625ad203. Accessed 4 Aug 2023
34. A. Martin, S. Harbison, K. Beach, P. Cole, An introduction to radiation protection. Introd. Radiat. Prot. (2018). https://doi.org/10.1201/9780429444104
35. The official FLUKA site: FLUKA Online Manual. http://www.fluka.org/fluka.php?id=man_onl. Accessed 4 Aug 2023.
36. T.T. Böhlen et al., The fluka code: developments and challenges for high energy and medical applications. Nucl. Data Sheets **120**, 211–214 (2014). https://doi.org/10.1016/J.NDS.2014.07.049
37. T. Goorley et al., Initial MCNP6 release overview. Nucl. Technol. **180**(3), 298–315 (2012). https://doi.org/10.13182/NT11-135
38. S. Agostinelli et al., Geant4—a simulation toolkit. Nucl. Instrum. Methods Phys. Res. Sect. A Accel. Spectrometers, Detect. Assoc. Equip. **506**(3), 250–303 (2003). https://doi.org/10.1016/S0168-9002(03)01368-8
39. S. E. Coleman, W. J. Zywiec, Validation of MCNP6.1 and MCNP6.2 using ENDF/B-VII.1 nuclear data for criticality safety application to plutonium and highly enriched uranium systems. Jun. 06, 2019.
40. M.B. Chadwick et al., ENDF/B-VII.1 Nuclear data for science and technology: cross sections, covariances, fission product yields and decay data. Nucl. Data Sheets **112**(12), 2887–2996 (2011). https://doi.org/10.1016/J.NDS.2011.11.002
41. V.P. Singh, S.P. Shirmardi, M.E. Medhat, N.M. Badiger, Determination of mass attenuation coefficient for some polymers using Monte Carlo simulation. Vacuum **119**, 284–288 (2015). https://doi.org/10.1016/J.VACUUM.2015.06.006
42. R. Biswas, H. Sahadath, A.S. Mollah, M.F. Huq, Calculation of gamma-ray attenuation parameters for locally developed shielding material: polyboron. J. Radiat. Res. Appl. Sci. **9**(1), 26–34 (2016). https://doi.org/10.1016/j.jrras.2015.08.005
43. J.H. Oh, S.H. Gwon, T.H. Kim, J.Y. Sun, S. Choi, Synthesis of titanium boride nanoparticles and fabrication of flexible material for radiation shielding. Curr. Appl. Phys. **31**(July), 151–157 (2021). https://doi.org/10.1016/j.cap.2021.08.009
44. M.E. Mahmoud, A.M. El-Khatib, M.S. Badawi, A.R. Rashad, R.M. El-Sharkawy, A.A. Thabet, *Fabrication, characterization and gamma rays shielding properties of nano and micro lead oxide-dispersed-high density polyethylene composites*, vol. 145 (Elsevier Ltd, Oxford, 2018). https://doi.org/10.1016/j.radphyschem.2017.10.017
45. E.A. Abdel Wahab, K.S. Shaaban, R. Elsaman, E.S. Yousef, Radiation shielding and physical properties of lead borate glass-doped ZrO_2 nanoparticles. Appl. Phys. A Mater. Sci. Process. **125**(12), 11–14 (2019). https://doi.org/10.1007/s00339-019-3166-8
46. V. Mani, N.S. Prasad, A. Kelkar, Ultra high molecular weight polyethylene (UHMWPE) fiber epoxy composite hybridized with Gadolinium and Boron nanoparticles for radiation shielding. Planet. Def. Sp. Environ. Appl. **9981**, 99810D (2016). https://doi.org/10.1117/12.2240135
47. E. Cheraghi, S. Chen, J.T.W. Yeow, Boron nitride-based nanomaterials for radiation shielding: a review. IEEE Nanotechnol. Mag. **15**(3), 8–17 (2021). https://doi.org/10.1109/MNANO.2021.3066390
48. R. Li, Y. Gu, Z. Yang, M. Li, Y. Hou, Z. Zhang, Gamma ray shielding property, shielding mechanism and predicting model of continuous basalt fiber reinforced polymer matrix composite containing functional filler. Mater. Des. **124**, 121–130 (2017). https://doi.org/10.1016/j.matdes.2017.03.045
49. A. Barabash, D. Barabash, V. Pertsev, D. Panfilov, Polymer-composite materials for radiation protection. Adv. Intell. Syst. Comput. **983**, 352–360 (2019). https://doi.org/10.1007/978-3-030-19868-8_36
50. M.R. Ambika, N. Nagaiah, S.K. Suman, Role of bismuth oxide as a reinforcer on gamma shielding ability of unsaturated polyester based polymer composites. J. Appl. Polym. Sci. **134**(13), 1–7 (2017). https://doi.org/10.1002/app.44657
51. O.A. Ersoz, F.Y. Lambrecht, H.M. Soylu, Tungsten-ethylene vinyl acetate (EVA) composite as a gamma rays shielding material. Indian J. Pure Appl. Phys. **54**(12), 793–796 (2016)
52. S.E. Gwaily, M.M. Badawy, H.H. Hassan, M. Madani, Natural rubber composites as thermal neutron radiation shields—I. B4C/NR composites. Polym. Test. **21**(2), 129–133 (2002). https://doi.org/10.1016/S0142-9418(01)00058-7
53. J. Pelto et al., Matrix morphology and the particle dispersion in HDPE nanocomposites with enhanced wear resistance. Polym. Test. **77**, 105897 (2019). https://doi.org/10.1016/j.polymertesting.2019.105897
54. M. Šupová, G.S. Martynková, K. Barabaszová, Effect of nanofillers dispersion in polymer matrices: a review. Sci. Adv. Mater. **3**(1), 1–25 (2011). https://doi.org/10.1166/sam.2011.1136
55. M. Rashad, H.O. Tekin, H.M. Zakaly, M. Pyshkina, S.A.M. Issa, G. Susoy, Physical and nuclear shielding properties of newly synthesized magnesium oxide and zinc oxide nanoparticles. Nucl. Eng. Technol. **52**(9), 2078–2084 (2020). https://doi.org/10.1016/j.net.2020.02.013
56. R. Li, Y. Gu, Y. Wang, Z. Yang, M. Li, Z. Zhang, Effect of particle size on gamma radiation shielding property of gadolinium oxide dispersed epoxy resin matrix composite. Mater. Res. Express (2017). https://doi.org/10.1088/2053-1591/aa6651
57. T.B. Martin, K.I.S. Mongcopa, R. Ashkar, P. Butler, R. Krishnamoorti, A. Jayaraman, Wetting-dewetting and dispersion-aggregation transitions are distinct for polymer grafted nanoparticles in chemically dissimilar polymer matrix. J. Am. Chem. Soc. **137**(33), 10624–10631 (2015). https://doi.org/10.1021/jacs.5b05291
58. M.I. Sayyed, N. Almousa, M. Elsafi, Preparation of mortar with Fe_2O_3 nanoparticles for radiation shielding application. Coatings (2022). https://doi.org/10.3390/coatings12091329
59. T. Özdemir, A. Güngör, I.K. Akbay, H. Uzun, Y. Babucçuoglu, Nano lead oxide and epdm composite for development of polymer based radiation shielding material: Gamma irradiation and attenuation tests. Radiat. Phys. Chem. **144**, 248–255 (2018). https://doi.org/10.1016/j.radphyschem.2017.08.021
60. M.I.I. Farnaz Nasehi, Evaluation of X and gamma-rays attenuation parameters for polyacrylamide and ZnO composites as light. J. Nucl. Med. Radiat. Ther. **10**(2), 1000404 (2019)
61. C.P. Li, C.Y. Kang, S.L. Huang, P.T. Lee, H.C. Kuo, F.C. Hsu, Near infrared radiation shielding using $CsxWO_3$ nanoparticles for infrared mini light-emitting diodes. Mater. Lett. **260**, 126961 (2020). https://doi.org/10.1016/j.matlet.2019.126961
62. X. Gan et al., Preparation of a CeO_2-nanoparticle thermal radiation shield coating on ZrO_2 fibers via a hydrothermal method. Ceram. Int. **43**(16), 14183–14191 (2017). https://doi.org/10.1016/j.ceramint.2017.07.161
63. L. Yu, P.L. Yap, A. Santos, D. Tran, D. Losic, Lightweight bismuth titanate (Bi4Ti3O12) nanoparticle-epoxy composite for advanced lead-free X-ray radiation shielding. ACS Appl. Nano Mater. **4**(7), 7471–7478 (2021). https://doi.org/10.1021/acsanm.1c01475
64. A. Hashim, K.H.H. Al-Attiyah, S.F. Obaid, Fabrication of novel (Biopolymer blend-lead oxide nanoparticles) nanocomposites: Structural and optical properties for low-cost nuclear radiation shielding. Ukr. J. Phys. **64**(2), 157–163 (2019). https://doi.org/10.15407/ujpe64.2.157

65. M.E. Mahmoud, R.M. El-Sharkawy, E.A. Allam, R. Elsaman, A. El-Taher, Fabrication and characterization of phosphotungstic acid—copper oxide nanoparticles—plastic waste nanocomposites for enhanced radiation-shielding. J. Alloys Compd. **803**, 768–777 (2019). https://doi.org/10.1016/j.jallcom.2019.06.290
66. O. Bawazeer et al., A review on using nanocomposites as shielding materials against ionizing radiation. J. Umm Al-Qura Univ. Appl. Sci. (2023). https://doi.org/10.1007/s43994-023-00042-9
67. K. Bagheri, S.M. Razavi, S.J. Ahmadi, M. Kosari, H. Abolghasemi, Thermal resistance, tensile properties, and gamma radiation shielding performance of unsaturated polyester/nanoclay/PbO composites. Radiat. Phys. Chem. **146**, 5–10 (2018). https://doi.org/10.1016/j.radphyschem.2017.12.024
68. S. Ganguly, P. Bhawal, R. Ravindren, N.C. Das, Polymer nanocomposites for electromagnetic interference shielding: a review. J. Nanosci. Nanotechnol. **18**(11), 7641–7669 (2018). https://doi.org/10.1166/jnn.2018.15828
69. A. Hashim, I.R. Agool, K.J. Kadhim, Novel of (polymer blend-Fe3O4) magnetic nanocomposites: preparation and characterization for thermal energy storage and release, gamma ray shielding, antibacterial activity and humidity sensors applications. J. Mater. Sci. Mater. Electron. **29**(12), 10369–10394 (2018). https://doi.org/10.1007/S10854-018-9095-Z/METRICS
70. R. Mehrara, S. Malekie, S.M.S. Kotahi, S. Kashian, Introducing a novel low energy gamma ray shield utilizing Polycarbonate Bismuth Oxide composite. Sci. Reports **11**(1), 1–13 (2021). https://doi.org/10.1038/s41598-021-89773-5
71. W. Huang, W. Yang, Q. Ma, J. Wu, J. Fan, K. Zhang, Preparation and characterization of γ-ray radiation shielding PbWO4/EPDM composite. J. Radioanal. Nucl. Chem. **309**(3), 1097–1103 (2016). https://doi.org/10.1007/S10967-016-4713-9/METRICS
72. T. Abdolahzadeh, J. Morshedian, S. Ahmadi, M. R. Ay, and O. Mohammadi, Introducing a novel Polyvinyl chloride/Tungsten composites for shielding against gamma and X-ray radiations. [Online]. http://irjnm.tums.ac.ir. Accessed 23 Jul 2023
73. J. Yin, W. Ma, Z. Gao, X. Lei, C. Jia, A review of electromagnetic shielding fabric, wave-absorbing fabric and wave-transparent fabric. Polymers (2022). https://doi.org/10.3390/polym14030377
74. L. Gholamzadeh, N. Asari-Shik, M.K. Aminian, M. Ghasemi-Nejad, A study of the shielding performance of fibers coated with high-Z oxides against ionizing radiations. Nucl. Instrum. Methods Phys. Res. Sect. A Accel. Spectrometers, Detect. Assoc. Equip. **973**, 164174 (2020). https://doi.org/10.1016/J.NIMA.2020.164174
75. S. Kilincarslan, I. Akkurt, I.S. Uncu, F. Akarslan, Determination of radiation shielding properties of cotton polyester blend fabric coated with different barite rate. Acta Phys. Polon. A Pol. Acad. Sci. (2016). https://doi.org/10.12693/APhysPolA.129.878
76. J.S. Son, S.C. Kim, Improving the density of functional fabrics to protect radiation workers in radiology departments. Coatings (2022). https://doi.org/10.3390/coatings12081142
77. H. Özdemir, B. Camgöz, Gamma radiation shielding effectiveness of cellular woven fabrics. J. Ind. Text. **47**(5), 712–726 (2018). https://doi.org/10.1177/1528083716670309
78. A. M. El-khatib, T. I. Shalaby, A. Antar, M. Elsafi, 340 Ali.Pdf (2022)
79. M. Afshar, J. Morshedian, S. Ahmadi, Radiation attenuation capability and flow characteristics of HDPE composite loaded with W, MoS 2, and B 4 C. Polym. Compos. **40**(1), 149–158 (2019). https://doi.org/10.1002/pc.24620
80. N. Jahan, W. Khan, A. Azam, A.H. Naqvi, Fabrication of transparent cellulose acetate/graphene oxide nanocomposite film for UV shielding. AIP Conf. Proc. (2016). https://doi.org/10.1063/1.4947715
81. H.A. El-Rehim, H. Kamal, E.S.A. Hegazy, E.S. Soliman, A. Sayed, Use of gamma rays to improve the mechanical and barrier properties of biodegradable cellulose acetate nanocomposite films. Radiat. Phys. Chem. **153**, 180–187 (2018). https://doi.org/10.1016/j.radphyschem.2018.08.007
82. F. El-Ashhab, L. Sheha, M. Abdalkhalek, H.A. Khalaf, The influence of gamma irradiation on the intrinsic properties of cellulose acetate polymers. J. Assoc. Arab Univ. Basic Appl. Sci. **14**(1), 46–50 (2013). https://doi.org/10.1016/j.jaubas.2012.12.001